Effect of stress and temperature on the optical phonons of aramid fibers

D. Bollas,[1,2] J. Parthenios,[1,2] and C. Galiotis[1,2,3,*]
[1]*Foundation for Research and Technology Hellas, Institute of Chemical Engineering and High Temperature Chemical Processes, Greece*
[2]*Inter-Departmental Programme of Graduate Studies in Polymer Science and Technology, University of Patras, Greece*
[3]*Materials Science Department, University of Patras, Greece*
(Received 7 December 2005; revised manuscript received 29 December 2005; published 3 March 2006)

The wave-number dependence upon stress and/or strain and temperature of two adjacent optical phonons of aramid fibers has been investigated. The results showed that both phonons soften considerably under axial tension. Experiments at various temperatures under fixed strain conditions have demonstrated that one of the phonons (ν_1=1611 cm^{-1}) is moderately anharmonic whereas the adjacent phonon (ν_2=1648 cm^{-1}) exhibits harmonic behavior. By modeling the fibers as one-dimensional molecular wires very good agreement between experiment and theory is obtained for the phonon temperature dependence under isostress conditions.

DOI: 10.1103/PhysRevB.73.094103 PACS number(s): 62.20.−x, 65.40.De

I. INTRODUCTION

The phonon anharmonicity of inorganic crystals has been extensively studied in the past.[1] In contrast there has been very limited work on the phonon anharmonicity of polymer crystals mainly due to the unavailability of relatively large polymer monocrystals for vibrational measurements. In fact, in a great number of cases the physical parameters of polymer crystals have been determined solely by molecular modeling.[2]

High-performance polymer fibers such as the poly (*p*-phenylene terephthalamide) (PPTA) hereafter referred as aramid, are ideal candidates for such kind of studies mainly due to (a) their highly "paracrystalline" order and (b) the high orientation of the macromolecular chains to the longitudinal- axial direction of the fiber.[3] In Fig. 1(a) the unit cell of the PPTA crystal is presented whereby the repeat unit of the molecular chain can be seen. Raman spectroscopy has been extensively used in the past as a tool for both the structural and mechanical characterization of aramids. In particular, the Raman vibrational modes recorded at the 1611 and 1648 cm^{-1}, hereafter referred to as phonons ν_1 and ν_2, respectively, shift to lower values under tension and to higher values under compression.[4–13] The first phonon corresponds mainly to ring/C—C stretching of the aromatic groups which are placed on the backbone of the molecular chain [Fig. 1(a)], while ν_2 corresponds mainly to amide/C=O stretching, which is a side group mode [Fig. 1(b)].[14] It has been shown that both phonons shift linearly as a function of the applied stress, whereas the shift of the ν_1 phonon is twice as large as that of the ν_2 phonon.[20] Thus, stress or strain calibration curves (phonon shift vs axial stress or strain) can be constructed, leading to a potential use of the aramid fibers as stress and/or strain sensors in composite materials.[6,8,20–23] This technique has already been employed successfully for the assessment of the stress transfer efficiency in aramid/epoxy composites under both tension and compression[15–18] and for the quantification of the stress concentration around circular notches in composite materials.[19]

In general, the interactions between vibrational modes of atoms, molecules, ions, or lattices affect certain physical properties of crystalline materials including polymers.[2] One way to probe these properties is to study the way the lattice vibration frequencies vary with temperature. In this respect, the temperature dependence of the ν_1 and ν_2 Raman phonons of a certain class of aramid fibers (Kevlar 29®) has been determined recently by Psarras *et al.*[22] The knowledge of the Raman shift with temperature of the bands of the two phonons, as above, would also allow their use as *in situ* temperature diagnostic tools. However, inverse stress and temperature measurements are problematic as the corresponding values of stress and temperature cannot be easily deconvoluted from a given wave-number shift. This manifests itself particularly in the case where axial stress measurements are conducted in composites that incorporate aramid fibers at elevated temperatures.

In this paper, we have conducted a systematic experimental study of the temperature dependence of phonons ν_1 and ν_2 shift of Kevlar 29® fibers in combination with uniaxial stress and strain measurements. In particular, the temperature dependence of the Raman bands of phonons ν_1 and ν_2 under either fixed strain or constant strain rate in tension has been measured, whereas the corresponding temperature dependence under fixed stress conditions has been derived. An explanation for the observed mode softening for phonon ν_1 and the corresponding mode hardening for phonon ν_2 with temperature under fixed axial strain is put forward. Finally, important conclusions are drawn for the degree of anharmonicity of the phonon potential energy wells within the 1600–1650 cm^{-1} wave-number range.

II. EXPERIMENT

The aramid fibers tested were as received Kevlar® 29 fibers produced by Du Pont de Nemours, USA. Details concerning the physical and mechanical properties of the fibers can be found elsewhere.[3,25] The experimental work involved the Raman spectra acquisition from the Kevlar® 29 fibers at different temperature levels under simultaneous tensile loading. The latter was carried out either (a) under a constant strain rate of deformation or (b) quasistatically, at fixed predefined strain levels.

For experiments (a) above, single Kevlar® 29 fibers were deformed at a strain rate of 0.04 in/in min on a Hounsfield H25KM loading frame equipped with a 20 N load cell, op-

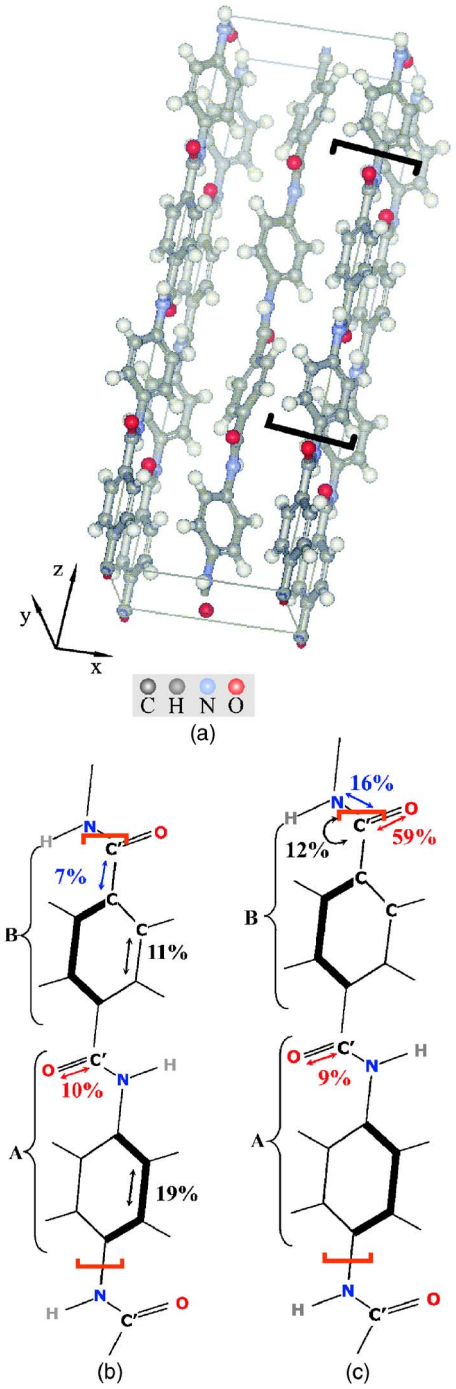

FIG. 1. (Color online) (a) The PPTA crystal unit[2] with the repeat unit of the molecular chain marked and (b) and (c) the origin of phonons ν_1 and ν_2, respectively, where the numbers (%) indicate the percentage contribution to the potential energy distribution (PED).[14]

erating at 5% of its dynamic range. The specimens were housed within a specially designed environmental chamber and the measurements conducted at constant temperature levels of 25 (ambient), 40, 60, 80, and 100 C. A schematic representation of the experimental setup used is shown in Fig. 2(a). The experimental procedure followed (gauge length, strain rate, etc.) were in accordance to the ASTM D3379 standard.[26] A minimum number of five fibers from the same bundle were tested at each temperature level.

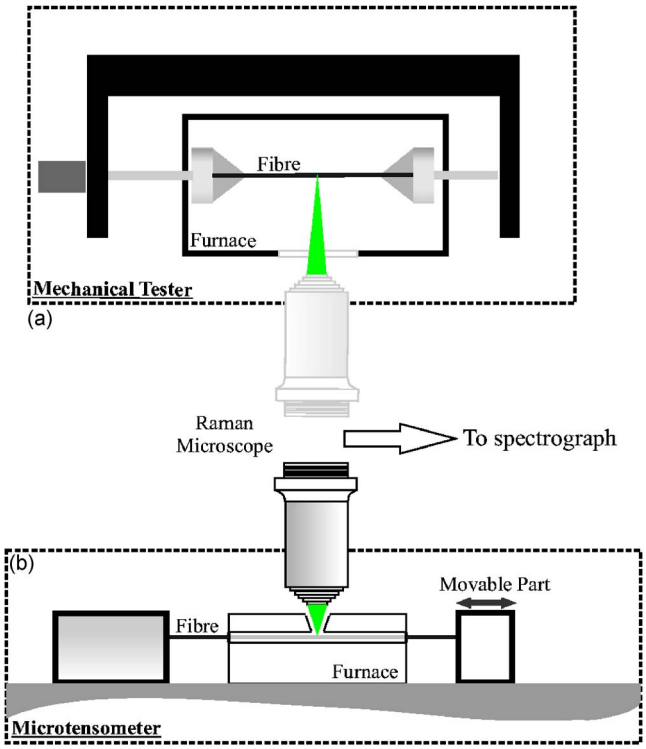

FIG. 2. (Color online) Schematic representation of the experimental setup used for the acquisition of Raman spectra under (a) a constant strain rate and (b) fixed strain levels.

For the (b) set of experiments, single Kevlar® 29 fibers were mechanically deformed stepwise at fixed strain levels of 0.2%, 0.5%, 0.8%, 1.0%, 1.5%, 2.0%, 2.5%, and 3.0% on a specially designed microtensometer [Fig. 2(b)] and at temperature levels of 25, 60, 80, 100, and 120 C. Again a minimum number of five fibers from the same bundle were tested at each temperature level, while five Raman spectra were recorded from each fiber at each strain level. Each fiber was carefully adhered on the jaws of the micrometer using a special cyano-acrylate based (type CC-33A, supplied by Kyowa, Japan) strain gauge cement. The gauge length of the fibers was 5.0 cm, which is short enough to avoid the twisting of the fiber during deformation. The strain was applied manually at the prefixed strain levels by moving the jaws of a tailor-made microjig with an accuracy of ± 1 μm, leading to an uncertainty in the applied strain of less than 0.002%. For heating the specimens a $4.0 \times 2.0 \times 2.0$ cm^3 handmade copper furnace was placed between the two parts of the microtensometer. The heating of the furnace was accomplished by means of 6 Resistors (MP930-20R-1%, RS Components Ltd, UK), connected in a series and fixed at both sides of the longer direction of the furnace. A cylindrical hole of 2.5 mm in diameter was drilled through the longer direction of the furnace and 5.0 mm from its top surface. At the center of the top surface a truncated cone opening was made allowing the focusing of the laser beam onto the fiber surface. The upper and lower diameter of the opening was 6.5 and 2.5 mm, respectively. It is worth adding here that a ceramic plate was surrounding the opening at the top of the furnace, to avoid

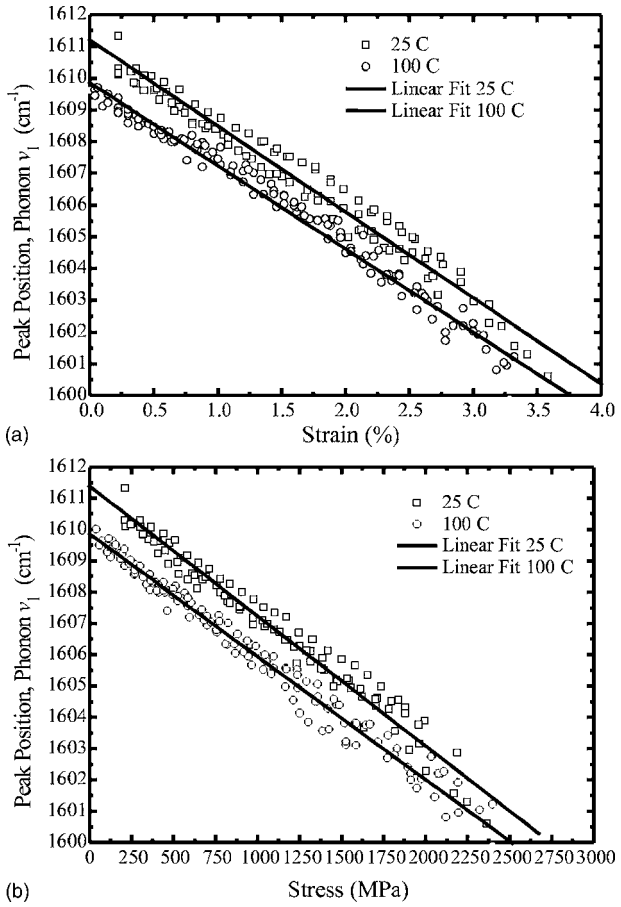

FIG. 3. The peak position of phonon ν_1 under a constant strain rate, as a function of applied (a) axial strain and (b) axial stress. For clarity only the results from the two extreme temperature levels of 25 and 100 C are given. The solid lines represent least-squares fits to the experimental data.

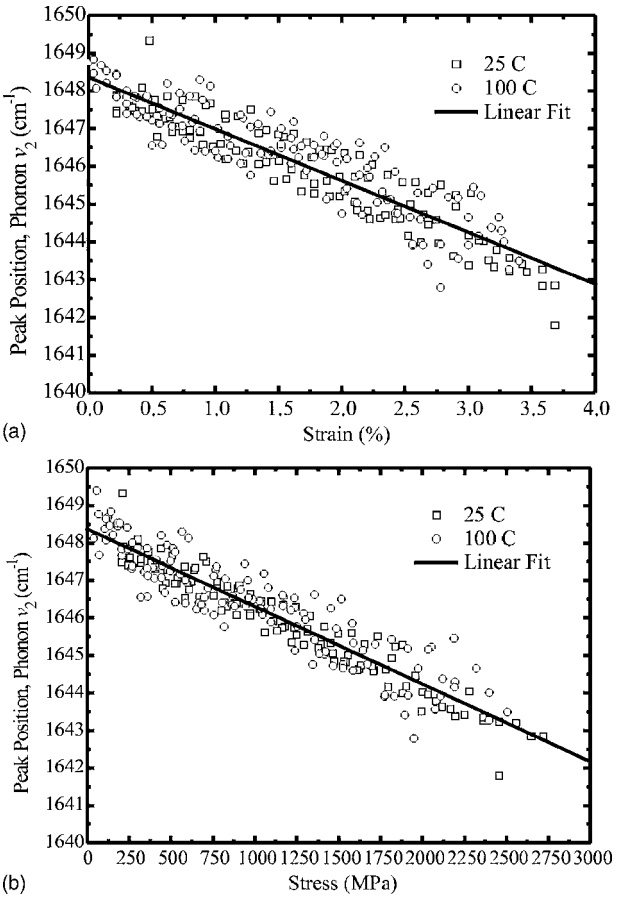

FIG. 4. The peak position of phonon ν_2 under a constant strain rate, as a function of applied (a) axial strain and (b) axial stress. For clarity only the results from the two extreme temperature levels of 25 and 100 C are given.

damaging the objective lens by the generated heat. Before conducting the experiments, the applied resistor current was calibrated in respect to temperature. This was necessary, since it was not possible to take temperature measurements during focusing the laser beam onto the fiber. The calibration procedure took place using a suitable thermocouple PT-100 (Omega Eng., UK) connected to a 61/2 Digit Multimeter (34401A, Agilent Technologies, USA) for monitoring thermocouple resistance changes at different levels of applied resistor's voltage. Thermocouple resistance was then converted to temperature using a calibration curve suitable for a PT 100 thermocouple.[27]

The Raman spectra were recorded by employing a remote Raman probe, designed in house and developed by Jobin Yvon/DILOR, France, (Model No. 5/23MFO, Dilor Ref. 1542). The microprobe uses an optical fiber for the Raman light collection, while the laser source has been incorporated into the main body of the microprobe. Laser source is a miniature diode pumped solid state laser (μGreen SLM, Uniphase) excited at 532 nm with 60 mW maximum output power. The use of a set of attenuating filters in front of the laser output mirror provides the capability of changing the incident laser power to the desired level of less than 1 mW on the specimen. The laser beam is first filtered through a microscope objective and a pinhole arrangement and is then directed to the microscope objective by reflection on the notch filter (O.D.=7). The 180° scattered light passes through the notch filter and guided through the optical fiber to a SPEX 1000M single spectrometer. The detector used was a Peltier cooled Charge-coupled device (CCD), Wright Instruments, UK (300×1200 pixels). It should be noted here that our experimental setup allows measurements of wavenumber positions from a given band with a repeatability of $\sim$1.0 cm^{-1}.[28] However, during the experiment at a fixed temperature of environment, shifts of individual Raman bands can be determined with an accuracy of $\sim$0.05–0.10 cm^{-1}. Detailed description of the remote Raman probe will be given elsewhere,[24] while a former version of it has been described in a previous work.[24]

III. RESULTS

A. Stress and strain dependence of ν_1 and ν_2 optical phonons of Kevlar® 29 at different levels of (constant) temperature under fixed strain rate

The phonon ν_1 dependence upon axial strain, ε_{zz}, and axial stress σ_{zz}, under a fixed strain rate is presented in Figs.

TABLE I. Stress and strain slopes for phonons ν_1 and ν_2 for different temperatures.

	Phonon ν_1			Phonon ν_2		
Temperature (C)	$\left(\frac{\partial \nu_1}{\partial \varepsilon_{zz}}\right)_T$ ($\mathrm{cm}^{-1}/\%$) (R^2)	$\left(\frac{\partial \nu_1}{\partial \sigma_{zz}}\right)_T$ (cm^{-1}/GPa) (R^2)	$\left(\frac{\partial \nu_1}{\partial \varepsilon_{zz}}\right)_T$ ($\mathrm{cm}^{-1}/\%$) (R^2)	$\left(\frac{\partial \nu_2}{\partial \varepsilon_{zz}}\right)_T$ ($\mathrm{cm}^{-1}/\%$) (R^2)	$\left(\frac{\partial \nu_2}{\partial \sigma_{zz}}\right)_T$ (cm^{-1}/GPa) (R^2)	$\left(\frac{\partial \nu_2}{\partial \varepsilon_{zz}}\right)_T$ ($\mathrm{cm}^{-1}/\%$) (R^2)
25	−2.81±0.07 0.96364	−4.08±0.05 0.97383	−2.86±0.04 0.99393	−1.42±0.07 0.80596	−1.97±0.10 0.81234	−1.30±0.07 0.99982
40	−2.74±0.07 0.92583	−4.23±0.07 0.96863		−1.23±0.08 0.72829	−2.04±0.09 0.77228	
60	−2.86±0.06 0.93418	−4.18±0.07 0.96142	−3.25±0.05 0.99732	−1.32±0.04 0.79841	−1.94±0.06 0.82894	−1.54±0.12 0.99722
80	−2.54±0.06 0.93466	−4.05±0.05 0.98044	−2.56±0.06 0.98653	−1.52±0.09 0.76498	−2.10±0.12 0.84808	−1.23±1.13 0.99494
100	−2.62±0.04 0.97721	−3.93±0.05 0.98192	−2.81±0.12 0.99339	−1.31±0.05 0.81245	−1.97±0.08 0.82060	−1.34±0.15 0.99287
120			−2.79±0.06 0.99858			−1.39±0.10 0.99740
Average values	−2.71±0.14	−4.09±0.13	−2.85±0.16	−1.36±0.15	−2.00±0.21	−1.36±0.26
Loading condition	Constant strain rate		Stepwise	Constant strain rate		Stepwise

3(a) and 3(b), respectively. In the actual figures only the results from the two extreme levels of temperature are presented to avoid data congestion. The slopes of the least-squares-fitted straight lines for all temperatures are given in Table I, with the R^2 values in all cases indicating satisfactory linear fits. As can be seen, the average value of $(\partial \nu_1/\partial \varepsilon_{zz})_T$ at different temperatures is approximately constant at -2.71 ± 0.14 $\mathrm{cm}^{-1}/\%$. Previous work[4,6] spanning over both tension and compression regimes has indicated that the $\nu = f(\varepsilon)$ function is best represented by a third degree polynomial; however, for purely tensile experiments[5] this can be overlooked for simplicity by fitting linear fits to the raw data at all temperatures. An average value of -4.09 ± 0.13 cm^{-1}/GPa is obtained out of all temperature levels for the slope of the phonon ν_1 shift in respect to the applied stress $(\partial \nu_1/\partial \sigma_{zz})_T$ and this conforms well with previous experiments conducted at room temperature.[20]

The phonon ν_2 dependence upon axial strain and stress under a fixed strain rate is presented in Figs. 4(a) and 4(b), respectively, and the corresponding least-squares-fitted slopes are given in Table I. Again, to avoid data congestion only the results from the two extreme levels of the temperature are presented. For the strain dependence $(\partial \nu_2/\partial \varepsilon_{zz})_T$, the values of the slopes present a greater scatter than those of phonon ν_1 but no systematic trend is observed, resulting to an average value of -1.36 ± 0.15 $\mathrm{cm}^{-1}/\%$. Regarding the phonon stress dependence $(\partial \nu_2/\partial \sigma_{zz})_T$, again no significant change per level of temperature is observed; an average value of -2.00 ± 0.21 cm^{-1}/GPa is obtained at all temperatures attempted here.

B. Strain dependence of ν_1 and ν_2 optical phonons of Kevlar® 29 at different levels of (constant) temperature at fixed strain levels

The dependence of phonon ν_1 upon axial strain at different levels of constant temperature but held at fixed strain levels is presented in Fig. 5(a). For reasons mentioned earlier only the results from the two extreme levels of temperature are presented. Concerning the strain dependence of this phonon, $(\partial \nu_1/\partial \varepsilon_{zz})_T$, the derived slopes of the least-squares-fitted straight lines for all temperature levels are given in Table I, while, once more, the R^2 values indicate satisfactory straight line fits. It is again clear that there are no significant differences between the slopes obtained at different temperatures with stepwise loading and the average value of $(\partial \nu_1/\partial \varepsilon_{zz})_T = -2.85\pm0.16$ $\mathrm{cm}^{-1}/\%$ is calculated.

The corresponding shift of the phonon ν_2 position with axial strain for stepwise loading and for all the applied temperature levels are shown in Fig. 5(b). The corresponding least-squares-fitted slopes are given again in Table I, with satisfactory R^2 values, and similar conclusions, as previously can be drawn with the results manifesting a much greater scatter than for phonon ν_1. The average value of $(\partial \nu_2/\partial \varepsilon_{zz})_T$, at fixed strain levels, is -1.36 ± 0.26 $\mathrm{cm}^{-1}/\%$ (Table I). It is worth noting here that each experimental point has been derived by 25 different Raman spectra. Thus, differences between the quality of each set of Raman spectra at each fixed strain level lead to differences in the lengths of the corresponding error bars.

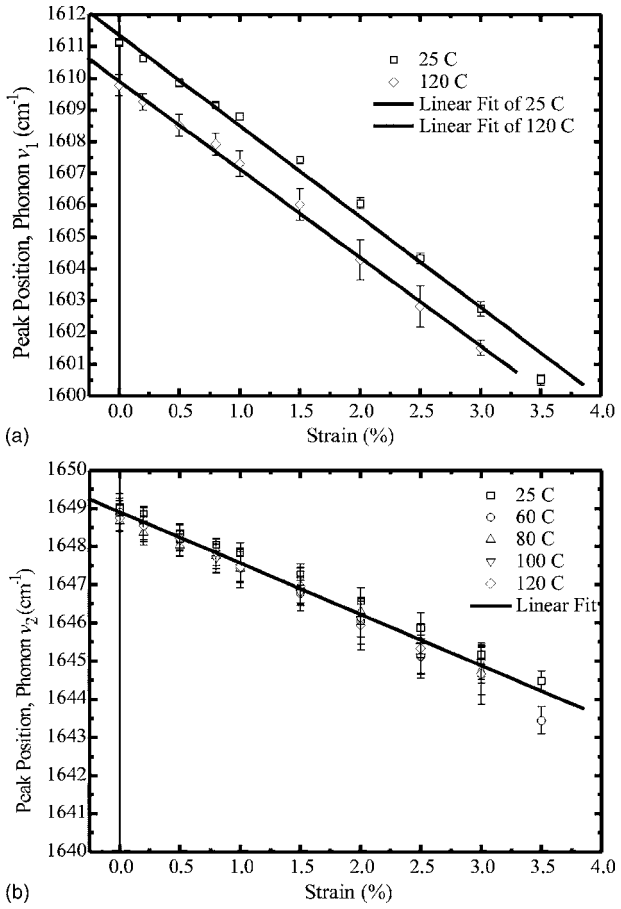

FIG. 5. The peak position of phonons (a) ν_1 and (b) ν_2, at various levels of temperature as a function of fixed applied strain levels. For clarity only the results from the two extreme temperature levels of 25 and 100 C are given in (a).

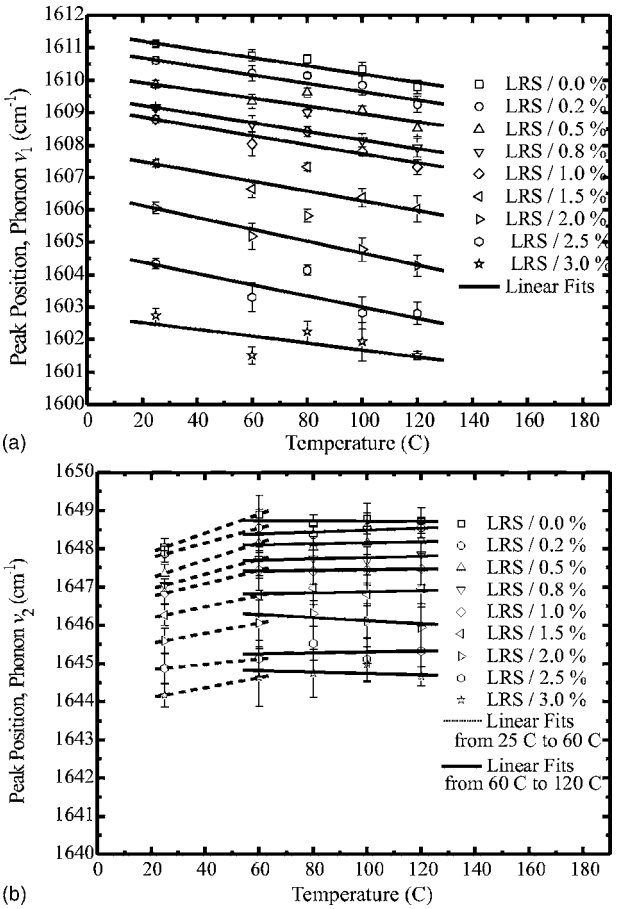

FIG. 6. The peak position of phonons (a) ν_1 and (b) ν_2, at fixed strain levels, as a function of temperature. The solid lines are least-squares fits to the raw data.

C. Temperature dependence of ν_1 and ν_2 optical phonons of Kevlar® 29 at different levels of (fixed) strain

The dependences of phonons ν_1 and ν_2 upon temperature at different fixed strain levels have been derived through the data of Figs. 5(a) and 5(b) and are shown in Figs. 6(a) and 6(b), respectively. As can be seen, the phonon ν_1 softens as a function of increasing temperature. The data show considerable scatter, nevertheless no significant differences are observed between individual sets of values for each strain level within experimental error. Assuming linear relationships for each strain level an average value of -0.0145 ± 0.0066 cm^{-1}/C is calculated for $(\partial\nu_1/\partial T)_{\varepsilon_{zz}}$. The relative high value of the wave-number vs temperature slope for phonon ν_1 indicates moderate anharmonicity for this particular vibration. In contrast, phonon ν_2 shows to be insensitive to temperature at least to the third decimal point for any $T>50$ C [Fig. 6(b)]. A statistical treatment (student t-test) of distinct sets of raw data also confirmed that the values of $(\partial\nu_2/\partial T)_{\varepsilon_{zz}}$ for all temperature levels are approximately zero with a certainty greater than 95%. There is, however, an indication as presented previously,[22] but also found here, that the overall temperature dependence from −50 to 150 C exhibits two distinct plateaus for which the slope of phonon ν_2 with temperature is -0.0014 ± 0.0003 cm^{-1}/C but with a sudden drop within the 25–50 C range (Fig. 7). As discussed later, the zero value of the slope for phonon ν_2 for any $T<25$ C and $T>50$ C indicates a harmonic vibration and differs markedly with the behavior of phonon ν_1.

IV. DISCUSSION

The slope of phonon wave-number shift as a function of applied strain or stress is an important parameter as it manifests the degree of alignment of a given vibration to the loading direction and, in addition, can provide information on the degree of mode softening or hardening of these phonons. The strain sensitivities of phonons ν_1 and ν_2, $(\partial\nu_1/\partial\varepsilon_{zz})_T$ and $(\partial\nu_2/\partial\varepsilon_{zz})_T$, respectively, measured in this work indicated moderate mode softening and appeared to be constant within the experimental error for the temperature range examined here (Table I). Similarly, the average values of $(\partial\nu_1/\partial\sigma_{zz})_T$ and $(\partial\nu_2/\partial\sigma_{zz})_T$ were also constant for all temperatures examined here. In general, the value of slopes for phonon ν_1 were twice as large as the corresponding values of phonon ν_2 and this indicates clearly the degree of alignment of the phenyl ring vibration to an applied axial stress or strain.

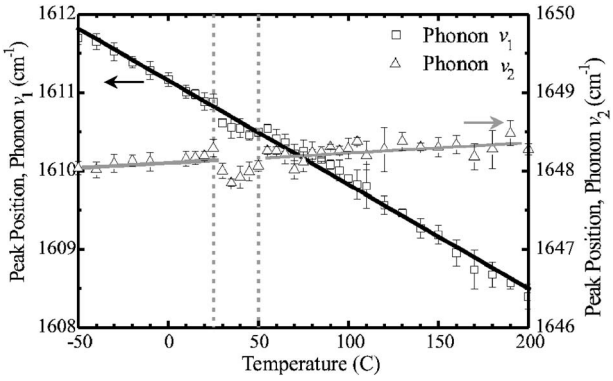

FIG. 7. Raman band peak position as a function of the temperature, for the ν_1 and ν_2 phonons.[22]

The total phonon wave-number shift $\Delta\nu_{k,tot}$ of Kevlar® 29 fibers is given by[22]

$$\Delta\nu_{k,tot}(\sigma_{zz},T)=\left(\frac{\partial\nu_k}{\partial\sigma_{zz}}\right)_{T=25}\Delta\sigma_{zz}+\left(\frac{\partial\nu_k}{\partial T}\right)_{\sigma_{zz}=0}\Delta T, \quad (1)$$

where σ_{zz} is the applied axial stress and T is the temperature. It is interesting to note that the first term of the equation represents the measured phonon dependence upon axial stress of the two phonons at RT and the second term refers to experiments conducted on free-standing fibers for which the axial stress was zero. The main question that has to be addressed here is whether the above equation (1) holds for any σ_{zz} and T, i.e.,

$$\Delta\nu_{k,tot}(\sigma_{zz},T)=\left(\frac{\partial\nu_k}{\partial\sigma_{zz}}\right)_{T}\Delta\sigma_{zz}+\left(\frac{\partial\nu_k}{\partial T}\right)_{\sigma_{zz}}\Delta T. \quad (2)$$

The results presented in Figs. 3(b) and 4(b), indicate clearly that the slopes of both phonons with respect to stress [first term of Eq. (2)] are constant for the range of temperatures tested here. The average values of the slopes are -4.09 cm^{-1}/GPa and -2.00 cm^{-1}/GPa for phonons ν_1 and ν_2, respectively. The moderate phonon softening with tensile stress confirms the initial premise that both vibrations have a strong axial character. It is interesting to add here that past work has shown[30] that at least for ambient temperature measurements, these slopes are also independent of the aramid fiber modulus and therefore can also be considered as the sensitivity to the applied stress of the PPTA crystal phonons.[6,31,32] Such behavior is characteristic of "equal-stress" (spring-in-series) solid bodies and, therefore, allows the study of the actual crystal under stress in crystalline or semicrystalline fibers.[6]

Regarding the second term of Eq. (2), it is noted that isostress measurements on thin fibers such as aramid are very difficult to conduct experimentally. In order to resolve this dependency and to throw further light into the nature of the two phonons we noted that previous work on inorganics has shown that in cubic or isotropic systems an isobaric phonon frequency shift with temperature arises from (a) sheer volume, V (implicit) contribution and (b) pure temperature, T (explicit) contribution.[29,33] In mathematical terms

TABLE II. Physical properties of aramid fibers (zz axis).

Physical properties of PPTA unit cell	
E_c (GPa)	220 (Ref. 35)
α_{zz}	-2.9×10^{-6} (Ref. 34)

$$\nu=\nu[V(T,p),T]\Rightarrow\left(\frac{\partial\ln\nu}{\partial T}\right)_p=\left(\frac{\partial\ln\nu}{\partial\ln V}\right)_T\left(\frac{\partial\ln V}{\partial T}\right)_p+\left(\frac{\partial\ln\nu}{\partial T}\right)_V,$$

where p is the applied hydrostatic pressure. We seek to apply the same principles to: (i) anisotropic crystalline fibers such as aramid, (ii) axial vibrational modes, and (iii) uniaxial stress measurements.

Indeed, a suitable way to do that is to represent thin anisotropic fibers as one-dimensional molecular wires. In this case, the isostress phonon frequency shift with temperature should arise from (a) length, l (implicit) contribution and (b) temperature, T (explicit) contribution:

$$\nu=\nu[l(T,\sigma_{zz}),T]\Rightarrow\left(\frac{\partial\ln\nu}{\partial T}\right)_{\sigma_{zz}}=\left(\frac{\partial\ln\nu}{\partial\ln l}\right)_T\left(\frac{\partial\ln l}{\partial T}\right)_{\sigma_{zz}}+\left(\frac{\partial\ln\nu}{\partial T}\right)_l,$$

or

$$\left(\frac{\partial\nu}{\partial T}\right)_{\sigma_{zz}}=\underbrace{\left(\frac{\partial\nu}{\partial\varepsilon_{zz}}\right)_T\left(\frac{\partial\varepsilon_{zz}}{\partial T}\right)_{\sigma_{zz}}}_{\text{implicit}}+\underbrace{\left(\frac{\partial\nu}{\partial T}\right)_{\varepsilon_{zz}}}_{\text{explicit}}. \quad (3)$$

For the PPTA crystal assuming linear stress strain for small deformations and constant axial thermal expansion coefficients for the range of temperatures applied here[34] we obtain from (3)

$$\left(\frac{\partial\nu}{\partial T}\right)_{\sigma_{zz}}=a_{zz}E_c\left(\frac{\partial\nu}{\partial\sigma_{zz}}\right)_T+\left(\frac{\partial\nu}{\partial T}\right)_{\varepsilon_{zz}}, \quad (4)$$

where E_c and α_{zz} are the axial crystal modulus and thermal expansion coefficient in the axial direction, respectively,[34,35] (Table II). The implicit effect (first term) refers to wave-number changes with temperatures due to changes in the interatomic separation. The explicit effect (second term) corresponds to the change in the population of energy levels with temperature and therefore is a direct reflection of bond anharmonicity; zero values would correspond to purely harmonic vibrations. The values of the unknown terms of Eq. (4) are given in Table III and, as can be seen, for the ν_1 phonon the effect of temperature (vibration amplitude) on the phonon wave number is dominant. For the ν_2 phonon both effects (length dependence and pure T) are weak within the

TABLE III. Implicit vs explicit effects for phonons ν_1 and ν_2.

Phonon (cm^{-1})	Implicit effect (length) (cm^{-1}/C)	Explicit effect (temperature) (cm^{-1}/C)	$\left(\frac{\partial \nu}{\partial T}\right)_{\sigma_{zz}}$ (cm^{-1}/C)	$\left(\frac{\partial \nu}{\partial T}\right)_{\sigma_{zz}=0}$ (cm^{-1}/C) (measured)
ν_1 (1611)	2.60×10^{-3}	-1.45×10^{-2}	-1.19×10^{-2}	-1.45×10^{-2} (Ref. 22)
ν_2 (1648)	1.30×10^{-3}	0.3×10^{-3}	1.6×10^{-3}	1.4×10^{-3} (Ref. 22)

60–120 C range examined here. By comparing the derived values of $d\nu/dT$ at constant stress with the experimentally derived values for $\sigma=0$ (Table III, Fig. 7) a satisfactory agreement is obtained. Hence, the initial premise that these fibers can be modeled as one-dimensional molecular wires appears to be valid. It is worth adding that, as seen in Fig. 7, the results for phonon ν_2 at zero stress confirm that its slope in respect to temperature is negligible for a much greater range of temperatures (−50 C–200 C). However, there is again an indication of a drop in wave numbers within the 25–40 C range. This anomaly to the overall observed trend is currently under investigation.

The corresponding total shift for combined stress and thermal fields for phonon ν_1 is now given [Eq. (2), Tables I and III] by

$$\Delta\nu_1 = -(0.0041\ \mathrm{cm}^{-1}/\mathrm{MPa})\Delta\sigma - (0.0119\ \mathrm{cm}^{-1}/\mathrm{C})\Delta T. \tag{5}$$

As is evident if the total shift is measured, the applied temperature can be derived only if the magnitude of the applied stress is known and vice versa. In other words, phonon ν_1 cannot be employed simultaneously as a stress and temperature sensor. The total shift for phonon ν_2 is given [Eq. (2), Tables I and III] by

$$\Delta\nu_2 = -(0.0020\ \mathrm{cm}^{-1}/\mathrm{MPa})\Delta\sigma + (0.0016\ \mathrm{cm}^{-1}/\mathrm{C})\Delta T. \tag{6}$$

In this case for any $\Delta\sigma > 100$ MPa and $\Delta T < 100$ C the phonon ν_2 can be used as a stress sensor with a confidence of about 90%. For any other combination, the knowledge of either stress or temperature is required for temperature or stress measurements, respectively.

The results presented here indicate significant differences between the two phonons both in terms of the degree of anharmonicity but also the type of bonding involved in each case. For the ν_1 phonon the effect of the change of interatomic spacing ("implicit" effect) on its wave-number shift is moderate but the anharmonicity factor ("explicit" effect) is relatively high and, thus, dominates the observed shift of wave numbers at fixed axial stress. Moreover, the dominance of the explicit effect indicates the presence of a strong covalent bonding and thus confirms the assignment of this peak as primarily due to the phenyl ring vibration. For the ν_2 phonon the effect of interatomic spacing is also moderate but its harmonic character (explicit effect of very low magnitude) at least for the range of temperatures examined here, is responsible for the very low-positive temperature sensitivity as compared to ν_1 phonon. Indeed in aramids this phonon emanates primarily from —C═O vibrations coupled to the polymer backbone but with the oxygen forming hydrogen bonds with the adjacent chain. It is indeed this electronic delocalization which is considered to be responsible for the "dilution" of the covalent bonding character of the ν_2 phonon.

V. CONCLUSIONS

Two adjacent optical phonons of aramid fibers have been investigated under combined thermal and mechanical fields. Both phonons soften considerably in tension under isothermal conditions by a fixed rate regardless of fiber modulus. Experiments conducted at a fixed strain at various temperatures (explicit effect) have demonstrated that phonon ν_1 is moderately anharmonic for the range of temperatures examined here (25–120 C). Phonon ν_2 differs considerably regarding thermal population effects (at equal strain) due to its harmonic character within the 50–120 C range examined here. By modeling the fibers as one-dimensional molecular entities the phonon dependence on interatomic separation with temperature (implicit effect) has also been derived and the results agree well with experiments conducted previously at zero stress. Both phonons appear to harden with temperature and this conforms well to what is expected from fibers with negative axial thermal expansion coefficient. Finally the total phonon wave-number dependence under isostress conditions is a function of both applied stress and temperature fields for phonon ν_1 whereas, for phonon ν_2, the effect of temperature is relatively weak.

ACKNOWLEDGMENTS

The authors would like to acknowledge Dr. G. C. Psarras for his contribution to the results presented in Fig. 7, the General Secretatiat of Research & Technology for financial support to D.B., and finally the Nanofun-Poly Network of Excellence of the European Communities for supporting the Research Group.

*Corresponding author. Email address: c.galiotis@iceht.forth.gr, galiotis@upatras.gr

[1] E. Anastassakis, H. C. Hwang, and C. H. Perry, Phys. Rev. B **4**, 2493 (1971); E. S. Zouboulis and M. Grimsditch, *ibid.* **43**, 12490 (1991); T. R. Hart, R. L. Aggarwal, and B. Lax, *ibid.* **1**, 638 (1970); M. Balkanski, R. F. Wallis, and E. Haro, *ibid.* **28**, 1928 (1983); J. Menendez and M. Cardona, *ibid.* **29**, 2051 (1984).

[2] R. E. Barker, J. Appl. Phys. **38**, 4234 (1967); Y. Wada, A. Itani, T. Nishi, and S. Nagai, J. Polym. Sci. A **7**, 201 (1969); T. G. Gibbons, J. Chem. Phys. **60**, 1094 (1974); M. Shen, Polym. Eng. Sci. **19**, 995 (1979); G. C. Rutlege and U. W. Suter, Polymer **32**, 2179 (1991); D. J. Laks and G. C. Rutdlege, Macromolecules **27**, 7197 (1994); J. A. O. Bruno, N. L. Allan, T. H. K. Barron, and A. D. Turner, Phys. Rev. B **58**, 8416 (1998).

[3] H. H. Yang, *Kevlar Aramid Fiber*, 1st ed. (Wiley, Chichester, 1993).

[4] C. Galiotis, in *Micromechanics of Reinforcement Using Laser Raman Spectroscopy; Microstructural Characterisation of Fiber-reinforced Composites*, edited by J. Summerscales (Woodhead Pub. Co., Cambridge, 1998), p. 224.

[5] R. S. Bretzlaff and R. P. Wool, Macromolecules **16**, 1907 (1983).

[6] C. Vlattas and C. Galiotis, Polymer **35**, 2335 (1994).

[7] C. Galiotis, Compos. Sci. Technol. **42**, 125 (1991).

[8] C. Galiotis, I. M. Robinson, R. J. Young, B. J. E. Smith, and D. N. Batchelder, Polym. Commun. **26**, 354 (1985).

[9] R. J. Young, D. Lu, and R. J. Day, Polym. Int. **24**, 71 (1991).

[10] M. C. Andrews and R. J. Young, J. Raman Spectrosc. **24**, 539 (1993).

[11] M. C. Andrews, R. J. Day, X. Hu, and R. J. Young, Compos. Sci. Technol. **48**, 255 (1993).

[12] M. C. Andrews, R. J. Day, X. Hu, and R. J. Young, J. Mater. Sci. Lett. **11**, 1344 (1992).

[13] W.-Y. Yeh and R. J. Young, Polymer **40**, 857 (1999).

[14] P. K. Kim, C. Chang, and S. L. Hsu, Polymer **27**, 34 (1986).

[15] J. Parthenios, D. G. Katerelos, G. C. Psarras, and C. Galiotis, Eng. Fract. Mech. **69**, 1067 (2002).

[16] H. Jahankhani and C. Galiotis, J. Compos. Mater. **25**, 609 (1991).

[17] C. Galiotis, Compos. Sci. Technol. **48**, 15 (1993).

[18] B. P. Arjyal and C. Galiotis, Adv. Compos. Lett. **4**, 47 (1995).

[19] B. P. Arjyal, D. G. Katerelos, C. Filiou, and C. Galiotis, Exp. Mech. **40**, 248 (2000).

[20] G. C. Psarras, J. Parthenios, and C. Galiotis, J. Mater. Sci. **36**, 535 (2001).

[21] J. Parthenios, G. C. Psarras, and C. Galiotis, Composites, Part A **32**, 1735 (2001).

[22] G. C. Psarras, J. Parthenios, D. Bollas, and C. Galiotis, Chem. Phys. Lett. **367**, 270 (2003).

[23] G. Anagnostopoulos, D. Bollas, J. Parthenios, G. C. Psarras, and C. Galiotis, Acta Mater. **53**, 647 (2005).

[24] J. Parthenios, D. Bollas, C. Dassios, D. G. Katerelos, and C. Koimtzoglou (unpublished); A. Paipetis, C. Vlattas, and C. Galiotis, J. Raman Spectrosc. **27**, 519 (1996).

[25] H. H. Yang, *Comprehensive Composite Materials* (Pergamon, Oxford, 2000), Chap. 1.

[26] Standard Test Method for Tensile Strength and Young's Modulus for High-Modulus Single-Filament Materials, Designation: D 3379-75 (Reapproved 1989).

[27] http://www.omega.com/temperature/Z/pdf/z252-254.pdf

[28] C. Filiou, C. Galiotis, and D. N. Batchelder, Composites **23**, 28 (1992); C. Filiou and C. Galiotis, Compos. Sci. Technol. **59**, 2149 (1999).

[29] E. Liarokapis, E. Anastassakis, and G. Kourouklis, Phys. Rev. B **32**, 8346 (1985).

[30] C. Vlattas, Ph.D. thesis, Materials Dept., Faculty of Engineering, Queen Mary College, University of London, 1995.

[31] I. M. Robinson, Ph.D. thesis, Materials Dept., Faculty of Engineering, Queen Mary College, University of London, 1987.

[32] C. Vlattas and C. Galiotis, Polymer **32**, 1788 (1991).

[33] P. S. Peercy, Phys. Rev. B **8**, 6018 (1973); J. Cai, C. Raptis, Y. S. Raptis, and E. Anastassakis, *ibid.* **51**, 201 (1995).

[34] T. Ii, K. Tashiro, M. Kobayashi, and H. Tadokoro, Macromolecules **19**, 1772 (1986).

[35] R. J. Young, S. J. Eichhorn, Y. T. Shyng, C. Riekel, and R. J. Davies, Macromolecules **37**, 9503 (2004).